Iran Polym J (2016) 25:787–797
DOI 10.1007/s13726-016-0467-z

ORIGINAL PAPER

Microwave-assisted green synthesis of hybrid nanocomposite: removal of Malachite green from waste water

B. S. Kaith[1] · Sukriti[1] · Jitender Sharma[1] · Tajinder Kaur[1] · Surbhi Sethi[1] · Uma Shanker[1] · Vidhisha Jassal[1]

Received: 11 May 2016 / Accepted: 1 August 2016 / Published online: 11 August 2016

Abstract Gum xanthan/psyllium-based nanocomposite was prepared by microwave-assisted synthetic method for the removal of toxic Malachite green (MG) dye from aqueous solutions. The nanocomposite was prepared by in situ incorporation of the $K_2Zn_3[Fe(CN)_6]\cdot 9H_2O$ nanoparticles into the semi-IPN matrix in the presence of ammonium persulphate and glutaraldehyde as initiator-crosslinker system. Liquid uptake efficacy of the hybrid superabsorbent was enhanced through the optimization of different reaction conditions, including APS = 0.027 mol L^{-1}; glutaraldehyde = 0.053 × 10^{-3} mol L^{-1}; solvent = 8.0 mL; acrylic acid = 10.928 mol L^{-1}; pH 7.0; reaction time = 60 s and microwave power = 100 % and its thermal behavior was evaluated using TGA-DTG-DTA technique. Candidate nanocomposite was characterized by FTIR, SEM, XRD and UV–visible spectroscopic methods. Various optimized parameters for the efficient removal (83 %) of the Malachite green were adsorbent dose of 800 mg, 14 mg L^{-1} initial dye concentration and contact time of 28 h. Further, Langmuir and Freundlich adsorption isotherms showed good applicability in adsorption process of MG onto the nanocomposite with maximum adsorption efficiency of 3.21 mg g^{-1}. However, for Freundlich isotherm, R^2 was around 0.9947 and value of 1/*n* was less than 1 for the synthesized nanocomposite which indicated that the Freundlich isotherm was more favorable than Langmuir isotherm model along with its usability for wide range of dye concentrations. The nanocomposite was found to be a potential product for dye removal from waste water and could prove to be a boon for textile sector.

Keywords Gum xanthan-psyllium · Superabsorbent · Nanocomposite · Malachite green · Textile sector

Introduction

Water is one of the resources with environmental, economic, social and political impact all over the globe. Nowadays, water contamination has become a serious environmental threat and has attracted the worldwide attention. Due to rapid industrialization and urbanization, toxic pollutants like metals, dyes, biodegradable wastes, phosphates, nitrates, hazardous and toxic chemicals, radioactive pollutants and pharmaceutical products are entering into the aquatic systems [1]. In India which is one of the largest producers and end users of dyes, most of the dyes consumed by industries, such as textile, dyeing, rubber, paper and pulp, tannery and paint lead to water pollution. The effluents discharged from such industries possess high chemical oxygen demand (COD) and biological oxygen demand (BOD), along with adverse impact on aquatic life which disturbs the natural equilibrium by reducing aquatic diversity and photosynthetic activity [2, 3].

Malachite green (MG), a basic cationic dye, has enormous industrial applications including papers, plastics, textile and pharmaceuticals [4, 5]. It is a stable nonbiodegradable dye and the presence of nitrogen in its complex aromatic structure makes it highly mutagenic and carcinogenic in nature [6]. Various physical and chemical techniques, such as precipitation, ion-exchange, coagulation and flocculation are employed to remove dyes from industrial effluents [7, 8]. Since these processes are not suitable for extremely soluble dyes [9, 10], therefore sorption is

✉ B. S. Kaith
bskaith@yahoo.co.in

[1] Research and Development Laboratory, Department of Chemistry, Dr B.R. Ambedkar National Institute of Technology, Jalandhar, Punjab, India

considered as most effective method for the treatment of industrial effluents [6, 11, 12].

Many polymer-based adsorbents have been developed for the treatment of dye-containing waste water. Modified and unmodified natural polymers are preferred, because they are cheap, easily available and eco-friendly in nature. Recently, modified polysaccharide-based nanocomposites are widely used as effective adsorbent materials for the effective removal of toxic dyes. Because of strong interaction between inorganic nanofillers and organic polymer matrices, hybrid nanocomposites exhibit increased surface area, hydrodynamic radius, improved thermal and mechanical properties [3, 13, 14].

Novelty of this work lies in the preparation of gel nanocomposite embedded with potassium zinc hexacyanoferrate (KZnHCF) nanoparticles and in the increase in its efficiency for the removal of carcinogenic textile dyes like Malachite green. Moreover, KZnHCF nanoparticles were prepared in the presence of eco-friendly natural surfactant *Sapindus mukorossi*. Sorption of Malachite green was found to be in better agreement with the Freundlich isotherm. Thus, this work deals with the preparation of an eco-friendly nanocomposite which can be used effectively for the treatment of textile industrial effluents without any adverse impact on the surrounding environment.

Experimental

Materials and method

Gum xanthan and psyllium were purchased from Sigma Aldrich and Sidhpur Sat-Isabgol Factory Gujarat, India, respectively. Glutaraldehyde and acrylic acid were obtained from Merck, India Ltd. *Sapindus mukorossi* was taken from Jalandhar market. Malachite green dye and ammonium persulphate were procured from SD Fine-Chem Ltd.

Synthesis of nanocomposites

In situ synthesis of nanocomposite was carried out by free radical polymerization technique. Equal amounts of gum xanthan and psyllium (1:1, w/w) were dissolved in 8.0 mL doubly distilled water in a reaction flask and 6.0 mL acrylic acid was added with constant shaking. The reaction mixture was kept undisturbed for about 4 h and a definite amount of potassium zinc hexacyanoferrate (KZnHCF) nanoparticles was imbibed in the soaked reaction mixture. This was followed by drop-by-drop addition of glutaraldehyde and ammonium persulphate while stirring the flask contents continuously. The reaction flask was kept in microwave for 60 s and the reaction was carried out under optimized reaction conditions. After the completion of reaction, the homopolymer was removed through extraction with water. The final product was dried in a hot air oven at 50 °C till constant weight was obtained.

Liquid uptake studies

Liquid uptake behavior of synthesized nanocomposite was studied at definite time intervals. A known amount of sample was immersed in 30 mL distilled water and the increase in weight was noted after every 4 h. Residual surface water was wiped-out using filter paper. The process was repeated until equilibrium was achieved.

The percentage swelling (P_s) was calculated as per Eq. (1) [15]:

$$P_s = \frac{W_s - W_d}{W_d} \times 100 \tag{1}$$

where, P_s = percentage swelling; W_s = weight of swollen sample; W_d = weight of dry sample.

Dye sorption studies

Adsorption equilibrium was studied for sorption of MG dye on the nanocomposite adsorbent with the help of UV–Vis spectrophotometer. The various process parameters such as adsorbent dose, contact time and initial concentration of dye solution were optimized with respect to percentage dye removal. Contact time was optimized by immersing 500 mg of nanocomposite in 50 mL aqueous dye solution (12 mg L^{-1}) and the graph was plotted by percentage dye removal versus contact time. Sorption of MG dye by the nanocomposite was studied at different time intervals of 4, 8, 12, 24 and 28 h by measuring the concentration of dye solution using an Agilent UV–Vis spectrophotometer. Efficiency of the nanocomposite for the sorption of MG dye from aqueous solution was calculated through Eq. (2) [16, 17]:

$$\text{Removal efficiency } (\%) = \frac{C_o - C_e}{C_o} \tag{2}$$

where, C_o = initial concentration (mg L^{-1}); C_e = equilibrium concentration (mg L^{-1}) of unabsorbed MG remained in aqueous solution.

Optimization of adsorbent dose was done by varying the amount of adsorbent from 400 to 800 mg at pre-optimized contact time. Dye concentration was varied between 12 and 20 mg L^{-1} to study the effect of dye concentration. Pre-optimized amount of nanocomposite was taken in 50 mL of MG dye solution. The adsorption of MG dye per unit mass of the adsorbent nanocomposite was calculated using Eq. (3) [16, 18]:

$$X_e = \frac{C_o - C_e}{W} \times V \tag{3}$$

where, X_e = equilibrium adsorption of MG per unit mass of adsorbent; V = volume of dye solution (L); W = weight of adsorbent.

Characterization

The graft copolymerization of polyacrylic acid chains onto the hybrid backbone and in situ incorporation of KZnHCF nanoparticles into synthesized polymer matrix were confirmed by different characterization techniques, including UV–visible (Agilent Cary 100 UV–Vis spectrophotometer), FTIR (Agilent Technologies Cary 630 spectrophotometer taken at 4000 to 400 cm^{-1} using KBr pellets), XRD (Broker AXS, X-ray diffractometer), SEM (LEO-435VF, LEO Electron Microscope) and transmission electron microscopy (TEM: Hitachi H-7500 instrument operating at 120 kV).

Thermal studies

Thermal behavior of the nanocomposite in relation to the polymer matrix and hybrid backbone was studied through TGA-DTA-DTG techniques in air at a heating rate of 10 °C min^{-1} on a SII EXSTAR 6000 TG/DTA 6300 system.

Results and discussion

Incorporation of polyacrylic acid chains onto hybrid backbone takes place through covalent bonding. –OH, –COOH, and $–CH_2$ functional groups are the active sites where grafting occurs. Moreover, during in situ synthesis of nanocomposite under pre-optimized reaction conditions, interaction between inorganic nanoparticles and the polymer matrix takes place both through primary and secondary bonding forces. Mechanism for the synthesis of nanocomposite is depicted in Scheme 1.

Optimization of various reaction parameters

To attain the maximum (690.8 %) liquid uptake efficacy, different reaction parameters optimized were APS = 0.027 mol L^{-1}; glutaraldehyde = 0.053 × 10^{-3} mol L^{-1}; solvent = 8.0 mL; acrylic acid = 10.928 mol L^{-1}; pH 7.0; reaction time = 60 s and microwave power = 100 % (Fig. 1).

It has been observed that initial increase in monomer, initiator and crosslinker concentrations resulted in increased liquid uptake capacity of the sample. However, after reaching the maximum liquid sorption capacity, further increase in the concentration resulted in decreased liquid sorption. This may be due to the predominance of homopolymerzation over graft copolymerization along

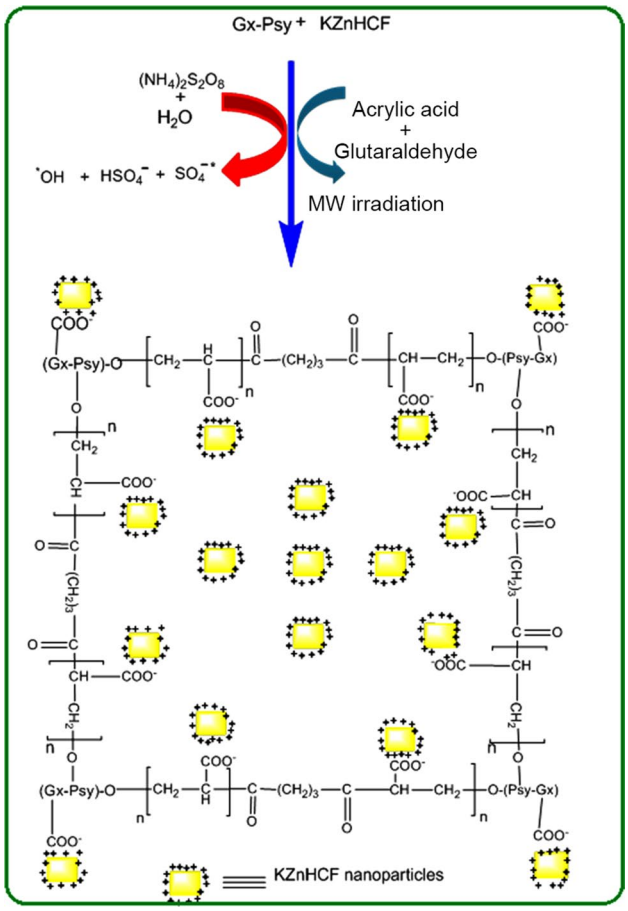

Scheme 1 Mechanism for the synthesis of hybrid nanocomposite

with intense-rigid structure formation with excess cross-linking, thereby resulting in decreased liquid sorption [19]. Volume of reaction medium was found to play an important role in attaining the maximum liquid uptake capacity. Initial increase in solvent volume resulted in easy approach of free radicals to the functional group of backbone and generation of active sites for grafting with polyacrylic acid chains. However, further increase in solvent volume beyond optimum liquid sorption decreased the concentration of free radicals, thereby resulting in less grafting and lower liquid uptake capacity [20]. Similarly, with initial increase in microwave power and reaction time there was an increase in liquid uptake. However, further increase in these parameters beyond optimum value resulted in reduced liquid uptake. This may be due to an excessive cross-linking on exposure to microwave for longer duration resulting in formation of a compact nanocomposite with lesser liquid uptake capacity [19].

Percentage liquid uptake was observed in different pH solutions ranging from 3.0 to 11.0, prepared by stock solutions of HCl and NaOH. Maximum liquid uptake of 690.8 % was observed at pH 7.0. However, lower sorption

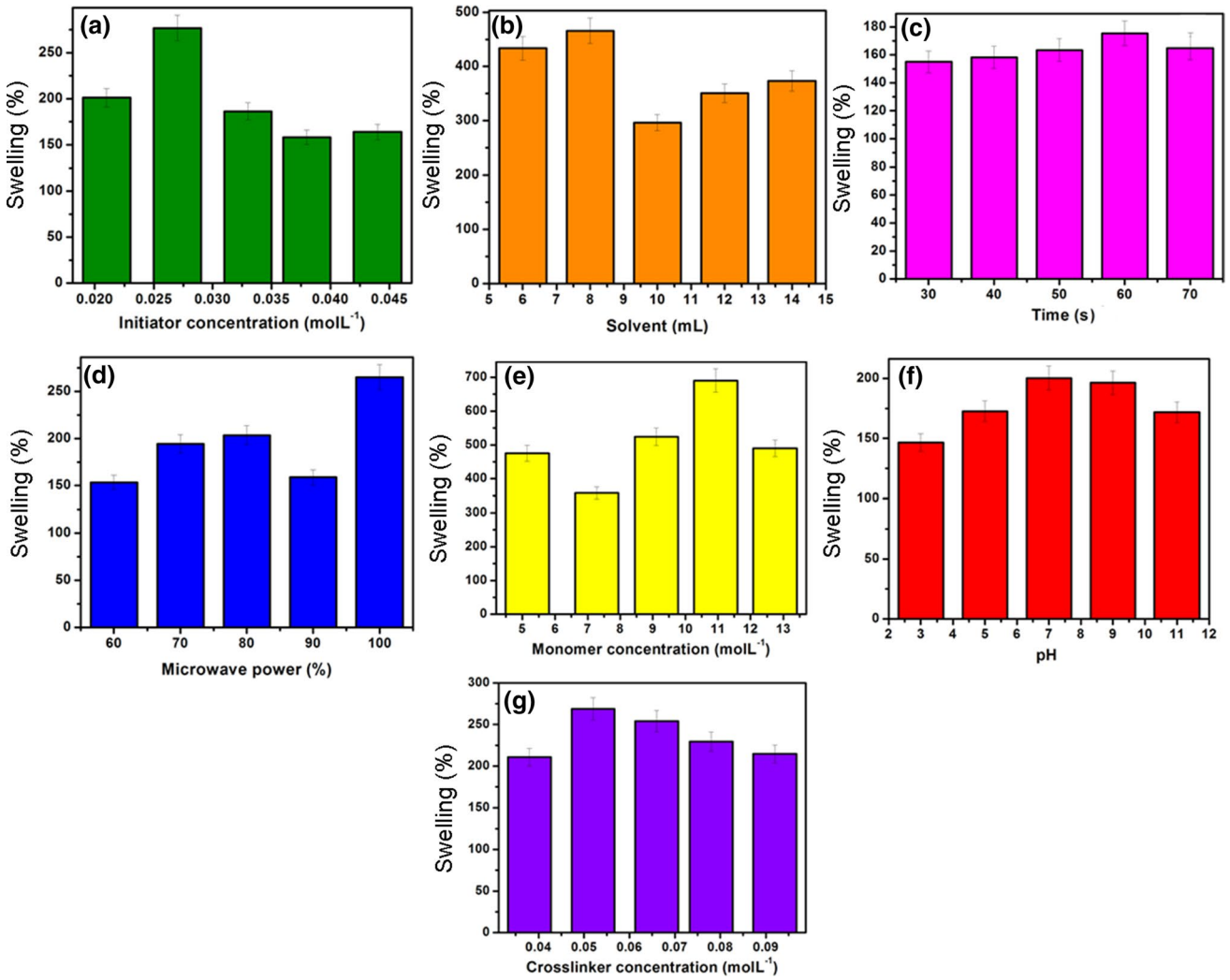

Fig. 1 Optimization of **a** initiator concentration; **b** reaction medium volume; **c** microwave time; **d** microwave power; **e** monomer concentration; **f** pH of the reaction medium; and **g** crosslinker concentration as a function of percentage swelling

was obtained in acidic and basic media (Fig. 1). This can be illustrated by osmotic pressure swelling theory described in Eq. (4) [21]:

$$\Pi_{\text{ion}} = RT\Sigma\left[C_{\text{g}} - C_{\text{s}}\right] \tag{4}$$

where, C_{g} = molar concentration of mobile ions in swollen sample; C_{s} = molar concentration of mobile ions in external fluid; R = universal gas constant; T = absolute temperature.

In neutral medium, more extensive polymeric structure was formed due to repulsions between different polymeric chains of synthesized superabsorbent, possessing $-COO^-$ groups resulting in increased liquid uptake. Thus, C_{s} has lower value as compared to C_{g} and has higher Π_{ion} value. In acidic medium, H^+ ions hindered the repulsion between $-COO^-$ groups present on polymeric chains which resulted in lower value of C_{g} and Π_{ion}. Similarly, in basic medium, the Na^+ ions produced a screening effect between the repulsing chains possessing $-COO^-$ groups leading to lower C_{g} and Π_{ion} value. Hence, lower liquid uptake was found under acidic and basic conditions.

Thermal studies

TGA of hybrid backbone showed different stages of decomposition with initial decomposition temperature (IDT) at 239.2 °C and final decomposition temperature (FDT) at 536.32 °C (Table 1). DTA showed exothermic decomposition at 471.7 °C (116.4 μV). DTG data exhibited rate of decomposition to be 1.81 mg min^{-1} at 283.6 °C and 0.34 mg min^{-1} at 480.2 °C.

The rate of decomposition of KZnHCF nanoparticles was slow under 101.3 °C and comparatively faster decomposition was observed in the range 101.3–421.2 °C with a mass loss of about 12.6 %. Thereafter, nearly 29 % mass loss was

Table 1 Thermogravimetric analysis of hybrid backbone, KZnHCF nanoparticle and nanocomposite

Sample code	TGA				DTA		DTG	
	IDT (°C)	1st stage decomposition, °C (%wt. loss)	2nd stage decomposition, °C (%wt. loss)	FDT (°C)	Exothermic peaks at different decomposition temperatures, °C (μV)		Decomposition temperature, °C (rate of wt. loss in mg min^{-1})	
					1st	2nd	1st	2nd
Hybrid backbone	239.8	239.8–303.9 (37.1 %)	303.9–536.7 (37.1 %)	536.7	286.2 (27.9)	471.7 (116.4)	283.6 (1.81)	480.2 (0.34)
KZnHCF nanoparticles	101.3	101.3–421.2 (12.6 %)	421.2–734.6 (29 %)	734.6	423.7 (0.13)	705.2 (0.070)	424.6 (0.329)	711.1 (0.159)
Nanocomposite	189.4	189.4–272.1 (30 %)	272.1–629.4 (60.7 %)	629.4	270.1 (−4.73)	513.8 (101.5)	260.7 (0.976)	410.2 (0.551)

IDT initial decomposition temperature, *FDT* final decomposition temperature, *TGA* thermogravimetric analysis, *DTA* differential thermal analysis, *DTG* differential thermogravimetric

observed from 420 to 734 °C, which could be attributed to the loss of cyanide moiety. The higher FDT of nanoparticles than the backbone can be explained on the basis of inorganic crystalline nature of the former [13]. DTA studies showed exothermic peak at 705.2 °C (0.070 μV) and rate of decomposition was found to be 0.329 mg min^{-1} at 424.6 °C and 0.159 mg min^{-1} at 711.1 °C.

In case of nanocomposites, IDT (204.7 °C) was found to be lower than that of backbone. However, FDT of nanocomposite was higher (630.7 °C). DTA analysis revealed exothermic peaks at 507.1 °C (131.2 μV). The rate of weight loss of nanocomposites was found to be 1.544 mg min^{-1} at 264.7 °C, which was lower than that of backbone. In case of hybrid backbone, KZnHCF nanoparticle and nanocomposite, DTA and DTG data have been found to support the TGA analysis, and hence were in conformity with TGA data.

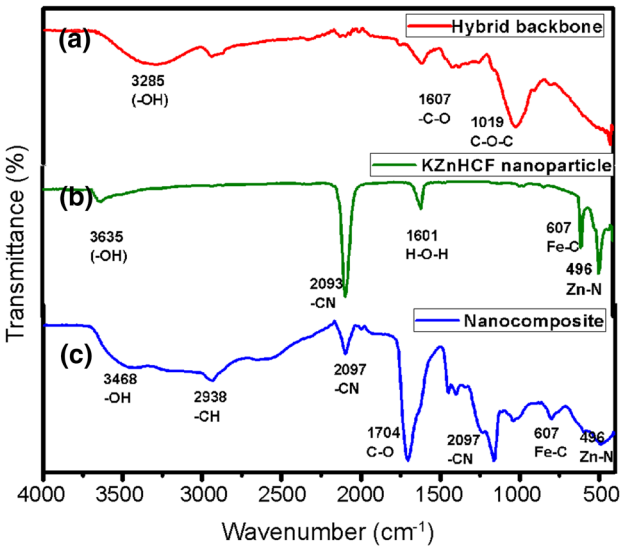

Fig. 2 FTIR spectra of **a** hybrid backbone; **b** KZnHCF nanoparticles; and **c** nanocomposites

Analysis of nanocomposite

FTIR spectroscopy

FTIR spectra of hybrid backbone, nanoparticle and nanocomposite are depicted in Fig. 2. In case of backbone, the main peaks were observed at 3285 (–OH stretching), 1706 (–C=O stretching) and 1019 cm^{-1} (C–O and C–O–C stretching vibrations), KZnHCF nanoparticles exhibited peaks at 3635 cm^{-1} due to the presence of –OH group, and at 2093 (–C≡N stretching), 1601 (H–O–H) bending, 597 (Fe–C stretching) and 498 cm^{-1} (Zn–N stretching) [22]. In case of nanocomposite, additional peaks were observed at 2938 (C–H stretching), 1704 (C=O stretching) and 1162 cm^{-1} (–C–O–C stretching) [13, 23, 24].

X-ray diffraction studies

The confirmation of the presence of KZnHCF nanoparticles in the polymer matrix was carried out through the powder X-ray diffraction studies (Fig. 3; Table 2). XRD pattern of KZnHCF nanoparticles, experimental interplanar spacing and relative intensity of the resultant compound were matched with JCPDS values (JCPDS card no. 33-1061) and the presence of KZnHCF particles was ascertained. Presence of sharp peaks indicated crystalline nature of nanoparticles [24]. XRD pattern of backbone depicted its semi-crystalline nature. However, grafting with polyacrylic acid chains and glutaraldehyde cross-linking resulted in increased crystallinity which further was enhanced on reinforcement with KZnHCF nanoparticles [25].

Scanning electron microscopy

Changes in the morphology of hybrid backbone were quite evident from SEM studies. SEM image of backbone

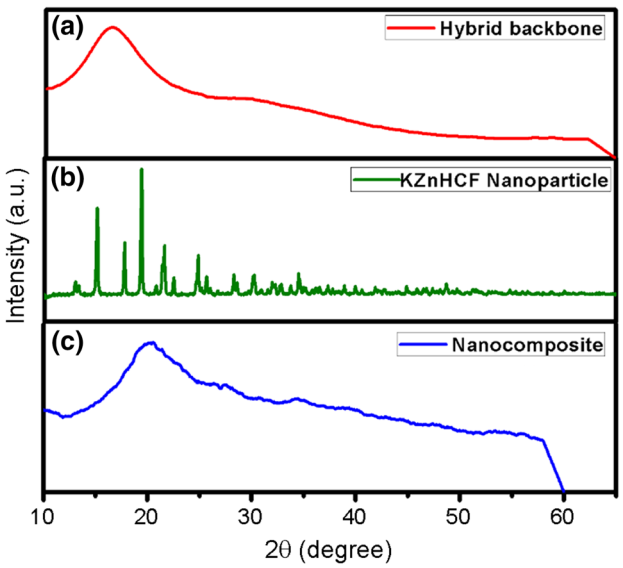

Fig. 3 XRD pattern of **a** hybrid backbone; **b** KZnHCF nanoparticles; and **c** nanocomposite

showed no deposition of polyacrylic acid chains and no cross-linking was observed. However, the SEM of nanocomposite revealed the cross-linking between polysaccharide chains of the hybrid backbone and grafted polyacrylic acid chains through glutaraldehyde along with the impregnated KZnHCF nanoparticles.

Grafting of polyacrylic acid chains onto hybrid backbone and cross-linking through glutaraldehyde resulted in physicochemical interactions between polyacrylic acid chains, polysaccharide chains of backbone and the crosslinker giving rise to the formation of three-dimensional network which was further strengthened through in situ incorporation of KZnHCF nanoparticles. All these physicochemical changes are quite evident from the SEM images of the synthesized nanocomposite. SEM images clearly indicated that morphological changes have taken place in the features of backbone after grafting, cross-linking and incorporation of nanoparticles (Fig. 4).

Transmission electron microscopy

The exact size and shape of KZnHCF nanoparticles were investigated using TEM. Cubic-shaped nanostructures with size ranging around 100 nm were found to be uniformly dispersed. Slight agglomeration was also observed [24] (Fig. 5)

Sorption studies of Malachite green dye onto nanocomposite

Adsorption mainly depends upon the nature of adsorbent. Adsorption capacity is directly related to the surface area of adsorbent which in turn affects the physicochemical properties. The synthesized nanocomposite showed higher adsorption capacity because of the presence of increased pore diameter and pore volume which ultimately resulted in increased surface area. Thus, nanocomposite was found to exhibit higher dye uptake capacity [20, 25].

Malachite green is a cationic dye carrying positive charge on nitrogen atom. This positively charged moiety undergoes ionic interaction with the anionic functional groups present on the nanocomposite resulting in dye removal from the aqueous solution. The greater degree of sorption of MG on the nanocomposite could also be explained on the basis of cation exchange process along with ionic interaction. Through cation–cation exchange process the MG dye molecules replace the positively charged entities of KZnHCF and undergo coordination with the $–COO^-$ groups of the polymer matrix. The faster cation exchange reactions and ionic interactions lead to more efficient removal of MG molecules from the solution. The mechanism of dye removal has been depicted in Scheme 2.

Optimization of different dye sorption parameters

Contact time

To calculate the shortest possible time for maximum removal of dye the contact time was optimized. Initially with increase in contact time the rate of dye removal was higher which was because of the availability of the active sites on the nanocomposite adsorbent [25]. About 67 % dye removal was observed in 12 h and maximum dye removal (82 %) was attained in 28 h (Fig. 6).

Adsorbent dose

Good adsorbents have the capacity to remove high amount of adsorbate at lower dose value. Optimum adsorbent dose

Table 2 XRD studies of hybrid backbone and nanocomposites

Sample code	2θ (degree)	β (FWHM) at 2θ-scale	Intensity (a.u.)	% Crystallinity
Hybrid backbone	18.08 ± 0.02	18.05 ± 0.08	528.5	53 ± 2.3
Nanocomposite	20.54 ± 0.06	32.12 ± 0.24	470.5	94 ± 1.7

FWHM full width half maxima

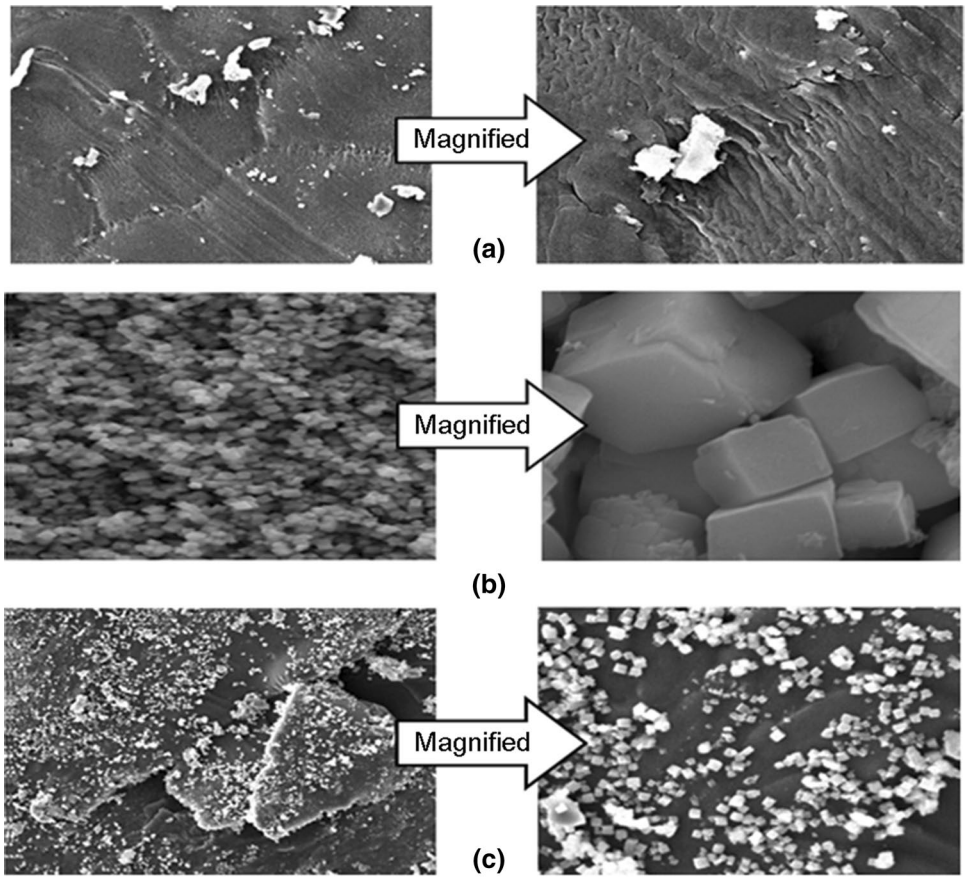

Fig. 4 SEM images of **a** backbone; **b** KZnHCF nanoparticles; and **c** nanocomposite

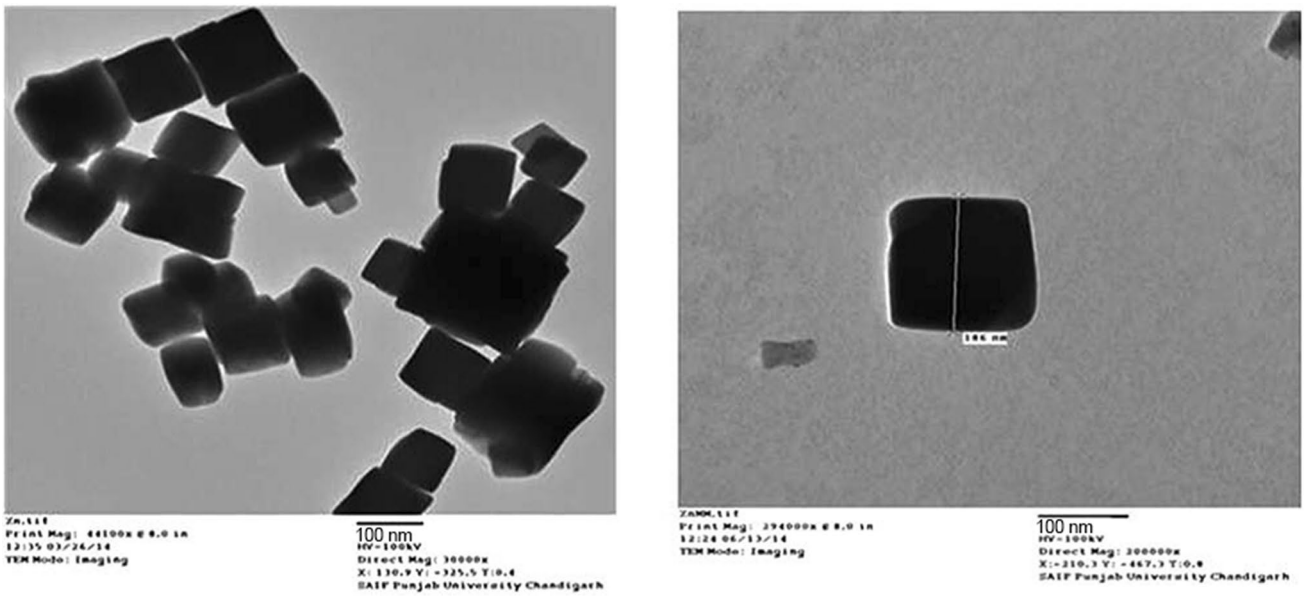

Fig. 5 TEM of KZnHCF Nanoparticles [24]

was found to be 800 mg with 83 % removal of MG dye. With increase in adsorbent dose there was proportionate increase in surface area with increased available active sites for adsorption through ionic interactions and cation–cation exchange. However, beyond the optimum adsorbent dose, reduction in dye removal was found which may be due to

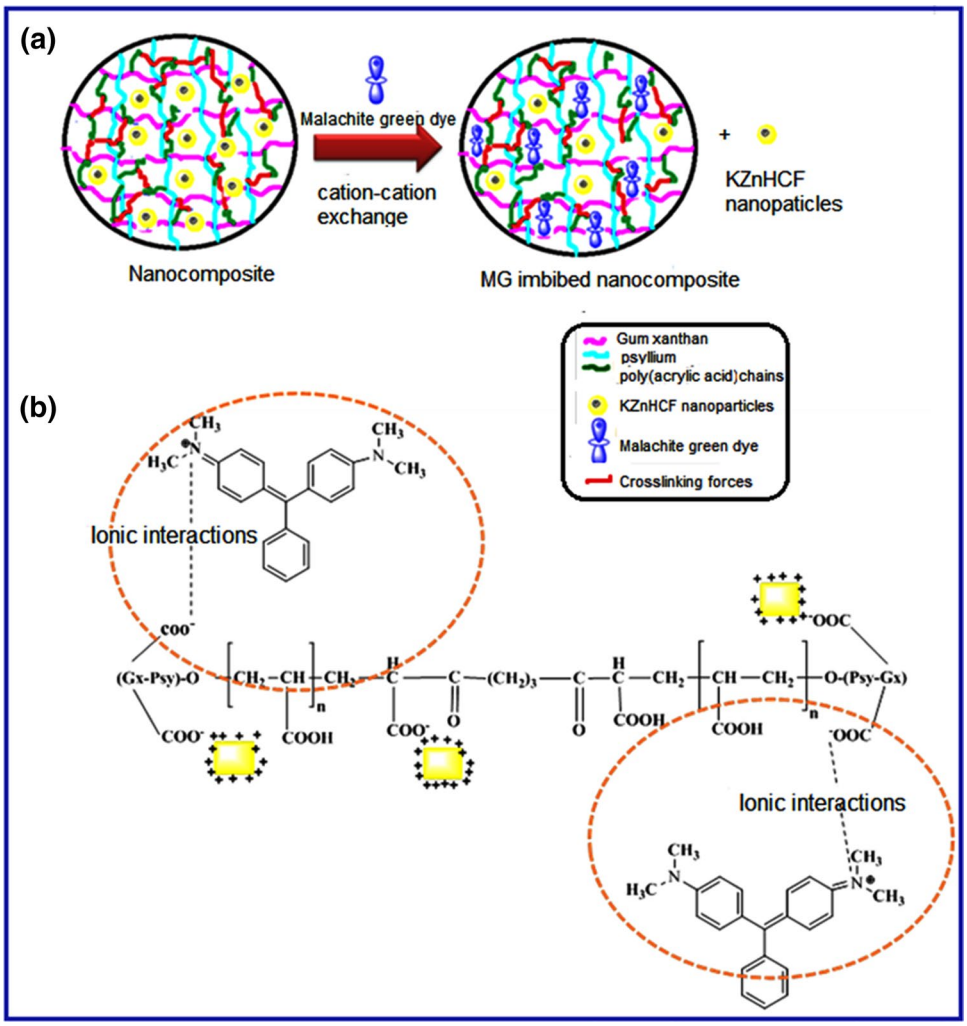

Scheme 2 Removal of Malachite green dye by nanocomposites: **a** cation–cation exchange; and **b** ionic interactions

the saturation of adsorption sites with MG dye molecules (Fig. 6) [12].

Initial dye concentration

Adsorption isotherms deal with the adsorption capacity of adsorbents for the adsorbates, analysis of adsorption equilibrium and degree of feasibility of adsorption process with respect to the initial concentrations. The variation of adsorption of MG dye onto adsorbent nanocomposite was studied with varying concentrations ranging from 12 to 20 ppm at ambient temperature. The optimum initial dye concentration was found to be 14 ppm. The mechanism of adsorption process at lower initial concentrations shows that a large number of sites are available to adsorbate and maximum adsorption occurs due to more solid–liquid physicochemical interactions. At higher initial concentrations, available adsorbent sites for adsorption become saturated and adsorption equilibrium is attained (Fig. 6). Thus, at lower initial concentrations, more number of dye molecules of the bulk solution are transferred to the surface of adsorbent nanocomposite and occupy maximum number of available sites, thereby favoring the adsorption process [12, 26, 27].

Adsorption isotherms

To study the adsorption behavior of adsorbate onto adsorbent, Langmuir adsorption isotherms and Freundlich adsorption isotherms were used in the present investigation for the removal of MG dye from waste water.

Langmuir adsorption isotherms

Langmuir adsorption mainly indicates the homogenous monolayer adsorption. Initially, adsorption on nanocomposite utilizes maximum number of available sites. Thus, adsorbent has a maximum level of liquid uptake capacity at adsorption equilibrium. Langmuir adsorption isotherm can be expressed by Eq. (5) [16, 28]:

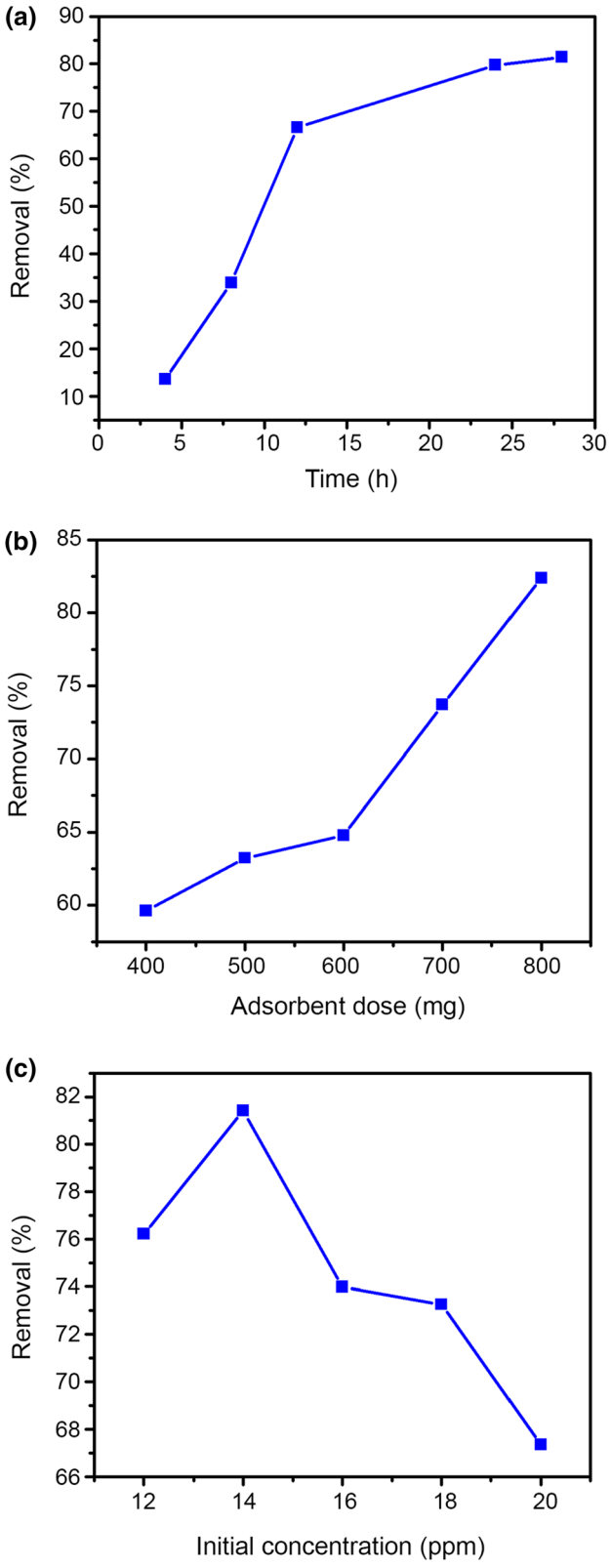

Fig. 6 Removal of MG dye: **a** optimization of contact time; **b** optimization of adsorbent dose; and **c** optimization of initial dye concentration

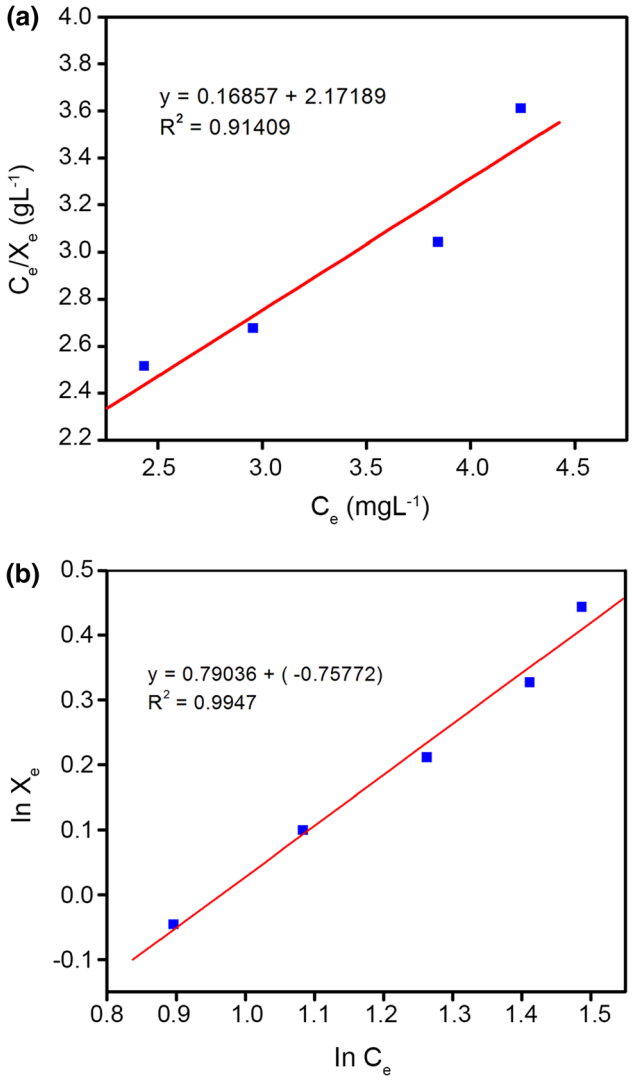

Fig. 7 Adsorption isotherm for adsorption of MG dye onto nanocomposites: **a** Langmuir adsorption isotherm; and **b** Freundlich adsorption isotherm

$$X_e = \frac{X_m \cdot b \cdot C_e}{1 + b \cdot C_e} \tag{5}$$

where, X_e = amount of adsorbed dye at equilibrium (mg g^{-1}); X_m = maximum adsorption capacity of the adsorbent; C_e = equilibrium concentration of the dye; b = Langmuir constant which relates with adsorption energy.

The essential characteristics of Langmuir isotherm is the monolayer adsorption of dye molecules on nanocomposite adsorbent and in terms of linear form can be expressed by Eq. (6) [22, 29]:

$$\frac{C_e}{X_e} = \frac{1}{X_m \cdot b} + \frac{C_e}{X_m} \tag{6}$$

From the graph of C_e/X_e vs. C_e, the values of Langmuir constant (b) and maximum adsorption capacity (X_m) can be calculated. For the adsorption of MG dye by the nanocomposite, value of b and X_m are found to be 4.16 L mg^{-1} and 3.21 mg g^{-1}, respectively. The correlation coefficient (R^2) was 0.91409 for Langmuir adsorption isotherm that depicted feasible adsorption behavior of MG dye onto nanocomposite (Fig. 7). Dimensionless constant called the separation term (R_L) was calculated to know feasibility of Langmuir adsorption isotherm using Eq. (7) [16]:

$$R_L = \frac{1}{1 + bC_o} \tag{7}$$

where, R_L = separation term, C_o = initial concentration of dye solution (mg L^{-1}). R_L values give the nature or behavior of uniform adsorption process, i.e., $0 < R_L < 1$: favorable; $R_L > 1$: unfavorable; $R_L = 1$: linear and $R_L = 0$: irreversible. The R_L values for the adsorption of MG dye on nanocomposite lie between 0 and 1 which indicates that Langmuir adsorption isotherm follows a favorable adsorption process [22].

Freundlich adsorption isotherm

Freundlich adsorption isotherm is obeyed by the adsorptions where the adsorbate forms a multi-molecular layer on the surface of the adsorbent. It means nonuniform distribution of MG dye molecules on the heterogeneous surface of nanocomposite adsorbent. The Freundlich isotherm can be represented by Eq. (8) [30]:

$$X_e = K_F \cdot C_e^{1/n} \tag{8}$$

where, X_e = equilibrium amount of dye adsorbed per unit mass of the adsorbent (mg g^{-1}); K_F = Freundlich isotherm constant; C_e = equilibrium dye concentration; n = dimensionless constant known as heterogeneity factor.

The linear equation for Freundlich isotherm in natural logarithm form can be given by Eq. (9) [31]:

$$\ln X_e = \ln K_F + \frac{1}{n} \cdot \ln C_e \tag{9}$$

From the plot $\ln X_e$ vs. $\ln C_e$, K_F and n can be calculated from intercept and slope of curve, respectively. From the graph of Freundlich isotherm, values K_F and n were 0.47 and 1.26, respectively, where R^2 comes to be around 0.9947 for nanocomposite indicating that this isotherm is more favorable in case of nanocomposite (Fig. 7). If $1/n > 1$, in that case adsorbent is usable for higher dye concentration. However, if $1/n < 1$ under such circumstances adsorbent is usable for entire range of dye concentration [32]. Therefore, the value of $1/n$ shows the applicability of the used adsorbent over the concentration range of the dye solution that gives significant importance to Freundlich adsorption isotherm. In case of the adsorption of MG dye on nanocomposite, $1/n$ is found to be less than 1, which specifies that the MG dye adsorption is totally applicable for a wide range of dye solution concentrations.

Conclusion

A novel nanocomposite of gum xanthan-psyllium as hybrid backbone was synthesized through in situ incorporation of KZnHCF nanoparticles which was evaluated for the removal of Malachite green dye from the aqueous medium. Langmuir and Freundlich adsorption isotherms showed good applicability to the adsorption process of MG onto the nanocomposite with maximum adsorption efficiency of 3.21 mg g^{-1}. Freundlich isotherm R^2 was around 0.9947 and value of $1/n$ was less than 1 for the synthesized nanocomposite, indicating that the isotherm was more favorable and clearly depicted multi-molecular layer adsorption of MG dye onto adsorbent surface along with its usability for a wide range of dye concentrations. The synthesized nanocomposite device can be of great importance from industry point of view.

Acknowledgments One of the authors is extremely thankful to MHRD for providing fellowship for carrying out this research work. The author is also thankful to IUAC, New Delhi, Instrumentation Center, IIT, Ropar, for characterization of the samples, and DST-FIST New Delhi for financial assistance in acquiring the FTIR and UV–Vis spectrophotometers at NIT Jalandhar.

References

1. Bonetto LR, Ferrarini F, De Marco C, Crespo JS, Guegan R, Giovanela M (2015) Removal of methyl violet 2B dye from aqueous solution using a magnetic composite as an adsorbent. J Water Process Eng 6:11–20
2. Bulut E, Ozacar M, Sengil I (2008) Adsorption of Malachite green onto bentonite: equilibrium and kinetic studies and process design. Micropor Mesopor Mat 115:234–246
3. Kushwaha AK, Gupta N, Chattopadhyaya MC (2014) Removal of cationic methylene blue and Malachite green dyes from aqueous solution by waste materials of *Daucus carota*. J Saudi Chem Soc 18:200–207
4. Garg VK, Kumar R, Gupta R (2004) Removal of Malachite green dye from aqueous solution by adsorption using agro-industry waste: a case study of *Prosopis cineraria*. Dyes Pigments 62:1–10
5. Mittal H, Jindal R, Kaith BS, Maity A, Ray SS (2015) Flocculation and adsorption properties of biodegradable gum-ghatti-grafted poly(acrylamide-*co*-methacrylic acid) hydrogels. Carbohyd Polym 115:617–628
6. Geetha P, Latha MS, Koshy M (2015) Biosorption of Malachite green dye from aqueous solution by calcium alginate nanoparticles: equilibrium study. J Mol Liq 212:723–730
7. Khankrua R, Pivsa-Art S, Hiroyuki H, Suttiruengwong S (2013) Thermal and mechanical properties of biodegradable polyester/silica nanocomposites. Energ Procedia 34:705–713

8. Jancar J, Douglas JF, Starr FW, Kumar SK, Cassagnau P, Lesser AJ, Sternstein SS, Buehler MJ (2010) Current issues in research on structure-property relationships in polymer nanocomposites. Polymer 51:3321–3343
9. Oladipo AA, Gazi M, Yilmaz E (2015) Single and binary adsorption of azo and anthraquinone dyes by chitosan-based hydrogel: selectivity factor and Box-Behnken process design. Chem Eng Res Des 104:264–279
10. Zhang YR, Wang SQ, Shen SL, Zhao BX (2013) A novel water treatment magnetic nanomaterial for removal of anionic and cationic dyes under severe condition. Chem Eng J 233:258–264
11. Shirsath SR, Patil AP, Bhanvase BA, Sonawane SH (2015) Ultrasonically prepared poly(acrylamide)-kaolin composite hydrogel for removal of crystal violet dye from wastewater. J Environ Chem Eng 3:1152–1162
12. Yagub MT, Sen TK, Afroze S, Ang HM (2014) Dye and its removal from aqueous solution by adsorption: a review. Adv Colloid Interface Sci 209:172–184
13. Ali SR, Chandra P, Latwal M, Jain SK, Bansal VK, Singh SP (2011) Synthesis of nickel hexacyanoferrate nanoparticles and their potential as heterogeneous catalysts for the solvent-free oxidation of benzyl alcohol. Chinese J Catal 32:1844–1849
14. Sharma K, Kumar V, Kaith BS, Kumar V, Som S, Kalia S, Swart HC (2015) Synthesis, characterization and water retention study of biodegradable gum ghatti-poly(acrylic acid-aniline) hydrogels. Polym Degrad Stab 111:20–31
15. Saruchi Kaith BS, Jindal R, Kumar V (2015) Biodegradation of gum tragacanth acrylic acid based hydrogel and its impact on soil fertility. Polym Degrad Stab 115:24–31
16. Kumar N, Mittal H, Parashar V, Ray SS, Ngila JC (2016) Efficient removal of rhodamine 6G dye from aqueous solution using nickel sulphide incorporated polyacrylamide grafted gum karaya bionanocomposite hydrogel. RSC Adv 6:21929–21939
17. Zhang Q, Zhang T, He T, Chen L (2014) Removal of crystal violet by clay/PNIPAm nanocomposite hydrogels with various clay contents. Appl Clay Sci 90:1–5
18. Khattri SD, Singh MK (2009) Removal of Malachite green from dye wastewater using neem sawdust by adsorption. J Hazard Mater 167:1089–1094
19. Sharma K, Kaith BS, Kumar V, Kalia S, Kumar V, Swart HC (2014) Water retention and dye adsorption behavior of Gg-cl-poly(acrylic acid-aniline) based conductive hydrogels. Geoderma 232–234:45–55
20. Sharma K, Kaith BS, Kumar V, Kumar V, Kalia S, Kapur BK, Swart HC (2014) A comparative study of the effect of Ni^{9+} and Au^{8+} ion beams on the properties of poly (methacrylic acid) grafted gum ghatti films. Radiat Phys Chem 97:253–261
21. Sharma K, Kumar V, Kaith BS, Kumar V, Som S, Kalia S, Swart HC (2014) A study of the biodegradation behaviour of poly(methacrylic acid/aniline)-grafted gum ghatti by a soil burial method. RSC Adv 4:25637–25649
22. Idris MN, Ahmad ZA, Ahmad MA (2011) Adsorption equilibrium of Malachite green dye onto rubber seed coat based activated carbon. Int J Basic Appl Sci 11:38–43
23. Banerjee C, Ghosh S, Sen G, Mishra S, Shukla P, Bandopadhyay R (2013) Study of algal biomass harvesting using cation in guar gum from the natural plant source as flocculant. Carbohyd Polym 92:675–681
24. Jassal V, Shanker U, Kaith BS, Shankar S (2015) Green synthesis of potassium zinc hexacyanoferrate nanocubes and their potential application in photocatalytic degradation of organic dyes. RSC Adv 5:26141–26149
25. Mahdavinia GR, Aghaie H, Sheykhloie H, Vardini MT, Etemadi H (2013) Synthesis of CarAlg/MMt nanocomposite hydrogels and adsorption of cationic crystal violet. Carbohyd Polym 98:358–365
26. Joseph F, Agrawal YK, Rawtani D (2013) Behavior of Malachite green with different adsorption matrices. Front Life Sci 7:99–111
27. Ahmad MA, Alrozi R (2011) Removal of Malachite green dye from aqueous solution using rambutan peel-based activated carbon: equilibrium, kinetic and thermodynamic studies. Chem Eng J 171:510–516
28. Kao S, Lin Y, Chin K, Hu C, Leung M, Ho K (2014) High contrast and low-driving voltage electrochromic device containing triphenylaminedendritic polymer and zinc hexacyanoferrate. Sol Energ Mat Sol Cells 125:261–267
29. Ayad MM, El-Nasr AA (2010) Adsorption of cationic dye (methylene blue) from water using polyaniline nanotubes base. J Phys Chem C 114:14377–14383
30. Baek M, Ijagbemi CO, Se-Jin O, Kim D (2010) Removal of Malachite Green from aqueous solution using degreased coffee bean. J Hazard Mater 176:820–828
31. Khan AA, Ahmad R, Khan A, Mondal PK (2013) Preparation of unsaturated polyester Ce(IV) phosphate by plastic waste bottles and its application for removal of Malachite green dye from water samples. Arab J Chem 6:361–368
32. Zhou C, Wu Q, Lei T, Negulescu II (2014) Adsorption kinetic and equilibrium studies for methylene blue dye by partially hydrolyzed polyacrylamide/cellulose nanocrystal nanocomposite hydrogels. Chem Eng J 251:17–24